A new optimization approach to enhance seismic performance of lead rubber bearing-isolated steel moment-resisting frames under extreme events

Jagajyoti Panda and Samit Ray-Chaudhuri*

Department of Civil Engineering, Indian Institute of Technology, Kanpur 208 016, India

This study presents an optimal design approach of lead rubber bearings (LRBs) for frame structures. The proposed approach involves a bi-objective optimization problem by maximizing the isolation efficiency along with minimization of peak bearing displacement. Further, a varying weight factor approach is proposed to target multiple performance objectives under different hazard levels of ground excitation. The optimal yield strength of LRBs for the considered frames is selected such that the total deviation of both objectives with respect to their specified limits is within 5%. Finally, it has been demonstrated that the proposed approach is generic in nature and valid for different superstructure flexibility and damping when subjected to ground motions of varying hazard levels.

Keywords: Bi-objective optimization, frame structures, ground motions, lead rubber bearings, optimal design, yield strength.

SEISMIC base isolation is a widely used passive control strategy to minimize earthquake-induced damage to structures. This is evident from the long list of important structures around the world that have been seismically isolated. Comprehensive reviews about different passive, semi-active and active isolation devices can be found in the literature[1,2]. Isolation devices based on elastomeric bearings shift the dominant frequencies of a structure away from the dominant frequencies of the ground motions, thus resulting in less force transfer to the superstructures during earthquakes[3,4]. For sliding bearing, force transfer is limited through the coefficient of friction of the sliding surfaces.

Lead-rubber bearing (LRB), an elastomeric passive device, has been used widely to protect important buildings, storage tanks, bridges and offshore structures[5,6]. LRBs basically consist of rubber layers with steel shims and have a lead plug inserted at the centre. High initial stiffness of LRBs is due to the presence of the lead plug, which also provides an elasto-plastic behaviour resulting in higher hysteretic damping of the isolated system during earthquakes[7,8]. Several studies have suggested that the intensity of ground motions may have varied influence on the outcomes of base-isolated structures[6,9]. As the behaviour of passive control devices such as LRBs is not adaptive, the performance of an isolated structure can be improved through the optimal selection of isolator parameters. Jangid[10] obtained the optimum yield strength of LRBs for near-fault ground motions. Zou[11], and Zou *et al.*[12] developed a numerical optimization technique to minimize the total cost of base-isolated buildings by considering peak inter-storey drift ratio (PIDR) of the superstructures and lateral displacement (PBD) of the LRB isolation system as the design performance criteria. Recently, Shinozuka *et al.*[13] have formulated a bi-objective optimization problem for a structure isolated by shape memory alloy-supplemented LRB (SMA-LRB). In the work of Shinozuka *et al.*[13], the problem statement was based on maximization of isolator efficiency along with minimization of bearing displacement.

The bilinear force–deformation behaviour of an LRB is characterized by parameters such as yield strength (F_y), yield displacement (q) and post-yield stiffness (K_{py}). To enhance the isolator efficiency, the present study calculates the optimum (F_y) of LRB by solving a bi-objective optimization problem involving both PIDR and PBD as independent objectives. The reason behind considering PIDR as an objective is that it provides reasonable information regarding the global dynamic instability and performance level of a structure. The optimal parameter of LRB is then evaluated for different hazard levels by varying the weight factor. Suitable weight factor for each objective is selected based on the principle of minimization of total error.

Numerical model

Structural model

To study the efficiency of the proposed approach for seismic isolation of existing older structures, a set of three

*For correspondence. (e-mail: samitrc@iitk.ac.in)

Table 1. Natural periods and modal masses of the considered frames

Frame	Mode no. 1		Mode no. 2		Mode no. 3	
	Period (s)	Modal mass (%)	Period (s)	Modal mass (%)	Period (s)	Modal mass (%)
Four-storey	0.74	93.93	0.23	5.35	0.12	0.81
Eight-storey	1.18	85.65	0.42	11.11	0.24	2.31
Sixteen-storey	1.85	81.34	0.66	12.5	0.38	3.47
Six-storey	1.17	82.7	0.39	13	0.21	3.9
Three-storey (brace frame (BF))	0.66	56.11	0.24	16.25	0.17	27.64

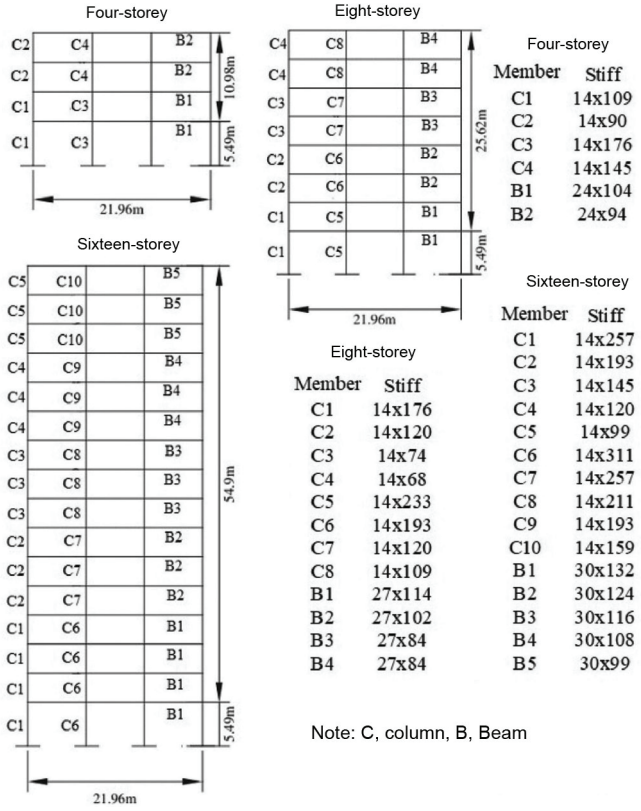

Figure 1. Schematic diagram of floor elevation of the representative steel moment-resisting frame structures.

pre-Northridge steel moment-resisting frame (SMRF) structures (an exterior frame for each of 4, 8 and 16-storey buildings) with the same plan dimensions was considered. These frames were designed and studied by Santa-Ana and Miranda[14]. As mentioned by the authors[14], these structures are representative of steel frame buildings existing in California, USA. Next, the effectiveness of the proposed approach was evaluated in contemporary code-designed structures by considering a six-storey SMRF (designed according to the provisions of FEMA-451 (ref. 15)) and a three-storey brace frame (a representative model of SAC Phase II structure in Los Angeles, USA)[16].

For the three pre-Northridge SMRF structures, the structural members from each building were designed by varying the stiffness such that Santa-Ana and Miranda[14] put the SMRF structures in the stiff category. Figure 1 shows the floor elevation of the exterior frames of these buildings along with the dimensions[14]. These frames were designed using the 1994 UBC-specified lateral load distribution for zone IV (ref. 17), and have a uniform mass and non-uniform lateral stiffness distribution with respect to height. The aforementioned pre-Northridge frames were modelled in OpenSees[18], an open source finite element platform. Figure 1 also gives the various sections considered for the structural members of these frames. All beam and column elements were modelled as 'beam-WithHinges' with a kinematic hardening ratio of 3% and P-delta coordinate transformation. A lumped mass of 16,000 kg was assigned to each node to simulate seismic mass on the frame and a Rayleigh damping of 2% was considered for the first two modes[9]. Table 1 provides the first three natural periods with modal masses from eigenvalue analysis. For all the buildings the normalized modal mass was found to be more than 80%, implying that the first mode is the dominant one.

The six-storey SMRF structure had a floor plan of 54.86 m along the east–west direction (six bays of 9.14 m each) and 42.67 m along the north–south direction (five bays of 8.53 m each). For this study, an appropriate numerical model of the exterior frame in the north–south direction (Figure 2 *a*) was developed in OpenSees[18], according to the details provided in FEMA-451 (ref. 15). The three-storey brace frame (BF) structure considered is a representative model of the SAC phase II structure in the Los Angeles area[16]. Similar to the aforementioned six-storey SMRF, an appropriate numerical model of the exterior frame in the north–south direction (Figures 2 *b*) was developed in OpenSees[18] according to the details provided in Hossain *et al.*[16]. The first three natural periods along with the normalized modal masses of the six-storey SMRF structure and three-storey BF structure were evaluated for the fixed-base conditions using eigenvalue analysis (Table 1).

Ground motion selection

For nonlinear time-history analyses of all the considered structures, a total of 40 ground motions (two bins with 20 motions each) from the SAC steel project representing

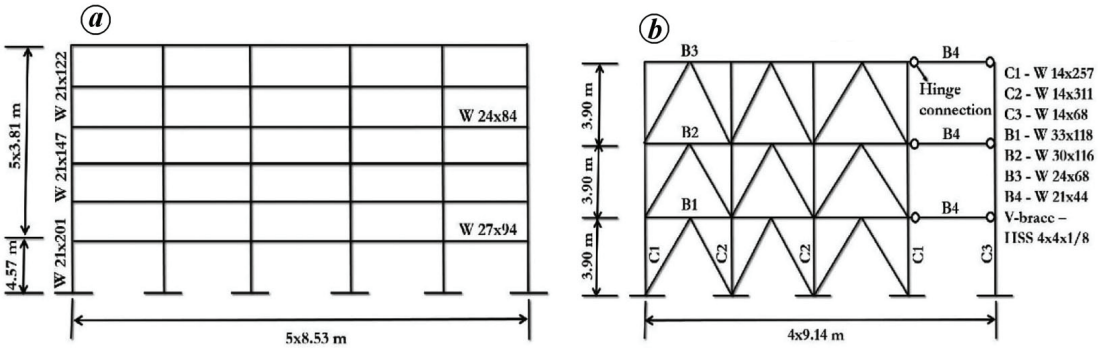

Figure 2. Schematic diagram of floor elevation along the N–S direction of (***a***) six-storey SMRF and (***b***) three-storey brace frame (BF) structures.

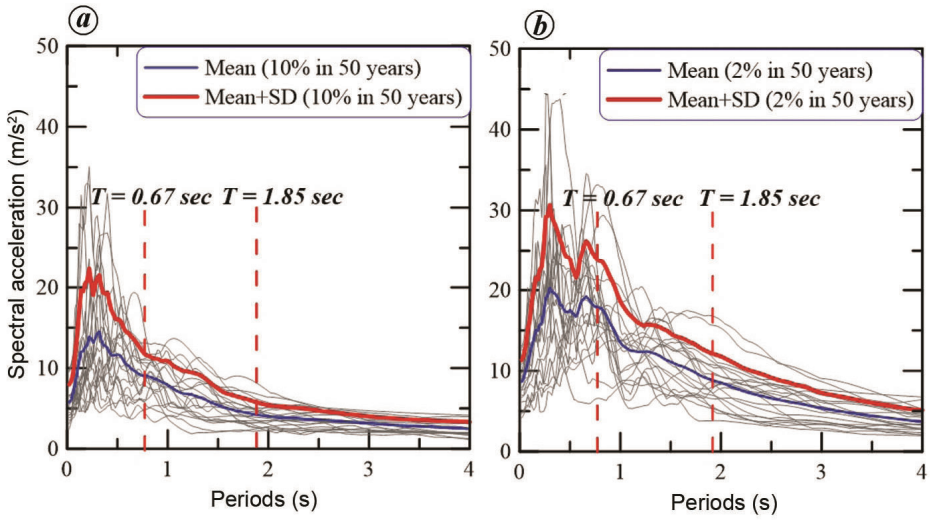

Figure 3. Mean and mean + SD acceleration response spectrum of the considered ground motions of hazard level: (***a***) 10% in 50 years and (***b***) 2% in 50 years.

hazard levels of 2% in 50 years and 10% in 50 years were considered[15,16,19]. Details of these motions can be found in Somerville *et al.*[19]. For both hazard levels, Figure 3 provides the mean response spectra (5% damping) of the motions along with the fundamental period range of the considered structures.

Isolator model

It is well known that LRB has a high initial stiffness (K_{Init}) before yielding of the lead plug and a low post-yield stiffness (K_{py}) due to the shear stiffness of rubber. Typical bilinear force–deformation behaviour of LRB (Figure 4 *b*) was effectively modelled in OpenSees[18] with 'elastomericBearingPlasticity' element available in the library. The element was developed by specifying K_{Init} in the local shear direction, the characteristic strength (Q) and post-yield stiffness ratio of the linear hardening component (α). According to Datta[3], and Skinner *et al.*[20], the characteristic strength (Q) of LRB is defined as

$$Q = q(K_{\text{Init}} - K_{\text{py}}), \tag{1}$$

where q is the yield displacement of LRB which depends on the height of the isolator. As $K_{\text{Init}}/K_{\text{py}} \approx 10$–$20$ (ref. 3), the Q value of LRB is almost equal to its yield strength F_{y}. Hence, in this study, the characteristic strength of the bearing was assumed as F_{y} while modelling the bearing element. The post-yield stiffness of LRB (K_{py}) leads to the post-yield isolation (fundamental) period T_{b} as

$$T_b = 2\pi\sqrt{M_R/K_{\text{py}}}, \tag{2}$$

in eq. (2), seismic mass $M_R = W_R/g$ with W_R being the total seismic weight on the bearing and g is the acceleration due to gravity. It may be noted that T_b, which is a representation of post-yield stiffness, is not the effective isolation period of the LRB isolated structures as usually defined in code provisions[21]. For bilinear isolators like LRB, the effective isolation period (T_{bs}) was assessed based on the

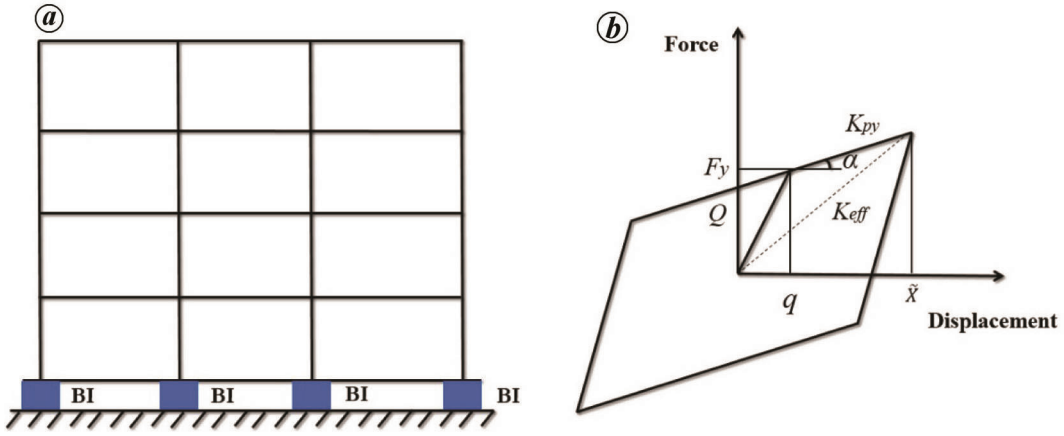

Figure 4. ***a***, Four-storey SMRF with lead rubber bearing (LRB) under each column. ***b***, Bi-linear behaviour of LRB with notations of the characteristic parameters.

equivalent stiffness of both the initial (K_{Init}) and post-yield (K_{py}) part depending on the design horizontal displacement of the isolator ($\tilde{X}$)[1,8]. In the axial direction, the bearing is defined using an elastic uniaxial material object with the vertical stiffness (K_{v}) and equivalent viscous damping (C_{v}) expressed as[3,8]

$$K_{\text{v}} = 6S_{\text{f}}^2 K_{\text{py}}, \tag{3}$$

$$C_{\text{v}} = 2\zeta_{\text{v}}\sqrt{M_R K_{\text{py}}}, \tag{4}$$

where ζ_{v} denotes the corresponding damping ratio. The shape factor (S_{f}) of the elastomer is characterized as the proportion of rubber area free to expand to the total loaded rubber area. In this study a value of 16 was considered for the seismic isolation bearings, which satisfies the specified design constraint that the rubber compressibility should be greater than 400 (refs 4, 8). Further, F_{y} was normalized with respect to W_R as $\bar{F}_{\text{y}}$ ($=F_{\text{y}}/W_R$), and T_b was normalized with respect to the fundamental period of the superstructure under fixed-base condition (T_s) as T_b/T_s for the subsequent analysis. The value of W_R was obtained from the reaction force by performing the gravity load analysis of the building under a fixed-base condition.

Rationale for considering inter-storey drift ratio as a performance parameter

The optimization problem in Jangid[10] was formulated by minimizing the force function $f(a_r, x_b)$ involving both peak horizontal roof acceleration (PHRA) of the structure (normalized and expressed as the variable a_r) as well as PBD (normalized and expressed as the variable x_b). This was to evaluate the optimum $\bar{F}_{\text{y}}$, where both objectives (i.e. a_r and x_b) are functions of $\bar{F}_{\text{y}}$. The problem statement was given by Jangid[10] as follows

$$f(a_r, x_b) = Q + 2K_{\text{py}}x_b + Ma_r, \tag{5}$$

the optimum $\bar{F}_{\text{y}}$ was evaluated by varying the fundamental time period of the superstructure. Further, the formulation to optimize the isolators was given by Shinozuka *et al.*[13] as follows

$$\text{Minimize}: f(\bar{F}_{\text{y}}) = \beta a_r(\bar{F}_{\text{y}}) + (1-\beta)x_b(\bar{F}_{\text{y}}). \tag{6}$$

The choice of weight factor (β) in the previously mentioned approaches was according to the considered hazard levels of ground motions used for the study. However, no emphasis was given in these works to PIDR, which is an excellent structural performance indicator.

To justify the importance of IDR in the optimization process, a numerical investigation following the constant weight factor (CWF) approach was performed in the present study with the aforementioned SMRF structures (Figure 1). Figure 4 *a* is a schematic diagram of a four-storey building having LRB as the isolator under each column. The steps adopted for the CWF approach were as follows:

(1) The mean and mean + SD estimations of PHRA, PIDR and PBD for a set of ground motions (representing a particular hazard level) were assessed for $0.02 \le \bar{F}_{\text{y}} \le 0.3$. These values were calculated for T_b/T_s of 2, 2.5 and 3 sec and q of 2.5 and 5 cm. The values of $\bar{F}_{\text{y}}$, T_b/T_s and q were adopted from Jangid[10].

(2) The values of $f(\bar{F}_{\text{y}})$ were calculated for each building from eq. (6) with $\beta = 0.75$ (as chosen by Shinozuka *et al.*[13]).

(3) The minimum value of $f(\bar{F}_{\text{y}})$ was chosen and the corresponding values of $\bar{F}_{\text{y}}$, PHRA, PIDR and PBD were also determined.

Based on the CWF approach, the evaluated values of optimum $\bar{F}_{\text{y}}$ were plotted against T_s for all buildings for ground motions of hazard level 10% in 50 years (Figure 5 *a*). For clarity of presentation, the points are joined by straight lines. Figure 5 *b* shows that the values of estimated

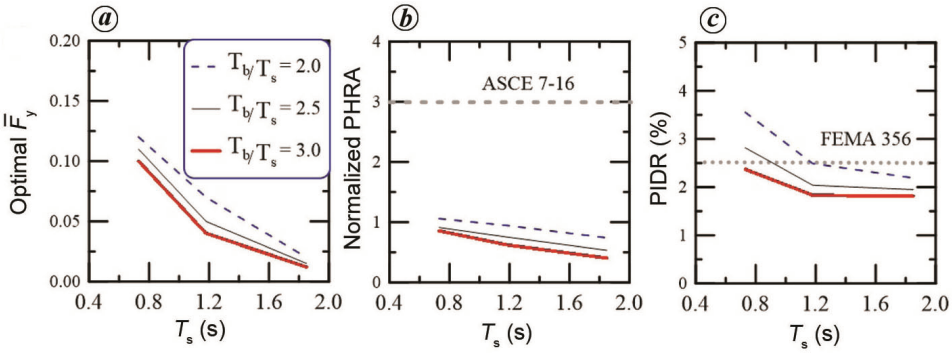

Figure 5. Variation of (***a***) optimum $\bar{F}_y$, (***b***) mean + SD values of normalized peak horizontal roof acceleration (PHRA) and (***c***) peak inter-storey drift ratio (PIDR) for hazard level 10% in 50 years using constant weight factor approach.

PHRA, normalized with respect to PGA, are found to be within the range 0.40–1.15, which is significantly below the code-specified design acceleration profile[17,21,22].

It may be noted that American Society of Civil Engineers 2016 (ref. 21) specifies horizontal acceleration profile along the height (i.e. $1 + 2z/h$, where z/h represents the normalized floor height) to characterize the seismic demand of nonstructural components for design purpose. However, PIDR varies significantly within this range of T_b/T_s (Figure 5 *c*). In fact, the PIDR values for all structures are well above the yield PIDR value of these frames. This observation can also be ascertained from the nonlinear static pushover analysis of the four-storey frame, where the maximum PIDR value is obtained as 2.66% against the yield roof displacement of 0.27 m. Therefore, it is clear that such an optimization scheme renders the isolator to be ineffective in reducing the vulnerability of the structure for ground motions of higher hazard levels as well. Furthermore, it is important to: (i) include PIDR as an objective and (ii) evaluate the effective range of T_b/T_s and q for an effective isolation design for such frame structures.

Proposed optimization scheme

Formulation

The objective of this study was to evaluate the optimum $\bar{F}_y$ of LRB that maximizes the isolation efficiency (i.e. reduce the vulnerability of the structure and nonstructural components) while minimizing the peak isolator displacement (i.e. reduce the damageability of the isolators). Ideally, the optimized design should cater to minimum economic loss arising due to seismic damage during the service life of any structure. However, estimation of annual economic loss (both direct and indirect) of a structure during its entire service life is a tedious process, which involves significant uncertainties in parameters such as site-specific hazards, intensity measures (IMs), engineering demand parameters (EDPs), damage measures (DMs), and item-wise cost estimate. Since the purpose of this study was to demonstrate the usefulness of variable weight factor approach, among others, for computational simplicity, we assume minimum economic loss for EDPs below DMs (taken as code-specified limits) and linear increment thereof. Further, for ease of computation, the cost associated with damage of structural, nonstructural components and isolators was assumed to be of the same order. This assumption eliminates the need of additional weight factors in the optimization problem.

To cover the damage of both structure and its nonstructural components, it may be desirable to include PHRA (as taken by previous researchers) as well as PIDR in the optimization scheme. However, as shown in the preceding sub-section, the influence of PHRA on the optimal design of the isolator is not significant for the pre-Northridge frames considered. Hence for those structures, the present study considers PIDR as the structural performance parameter for optimum design of the isolator to simplify the optimization scheme, as will be demonstrated here. The results of nonlinear analyses show that the variations of both objectives (i.e. for PIDR and PBD) are almost contradictory in nature. An improvement in one can only be achieved at the expense of the other, which actually makes sense as flexible bearings (resulting in higher PBD) reduce force transfer to the structure (i.e. lower PIDR). Therefore, the associated bi-objective optimization problem can be formulated as an equivalent single-objective problem by incorporating a weight factor (β) while considering $\bar{F}_y$ as the design variable. The formulation of the problem can be expressed as follows

$$\text{Minimize: } f(\bar{F}_y) = \beta d_r(\bar{F}_y) + (1-\beta)x_b(\bar{F}_y), \tag{7}$$

$$\text{Subjected to: } 0.02 \le \bar{F}_y \le 0.3, \tag{8}$$

where $d_r(\bar{F}_y)$ and $x_b(\bar{F}_y)$, both functions of $\bar{F}_y$, are the objectives of the optimal design problem, i.e. PIDR and PBD of the base isolated structure respectively.

From eq. (7), the relative importance of one objective with respect to the other can be determined by the weight factor β. Since PIDR and PBD have different units and magnitudes, to incorporate their variations in the optimal design formulation as given in eq. (7), the values of PIDR and PBD are normalized with respect to their maximum values (within the selected range of $\bar{F}_y$, as mentioned in eq. (8)) to scale them appropriately between 0 and 1. Thus, eq. (7) can be rewritten as

$$\text{Minimize: } f(\bar{F}_y) = \beta d_{rn}(\bar{F}_y) + (1-\beta) x_{bn}(\bar{F}_y), \tag{9}$$

$$\text{Subjected to: } 0.02 \le \bar{F}_y \le 0.3, \tag{10}$$

where $d_{rn}(\bar{F}_y)$ and $x_{bn}(\bar{F}_y)$ represent the normalized values of PIDR and PBD respectively.

Selection of weight factor

Selection of proper β for the optimal design of the isolator is important as it determines the relative weight of one objective with respect to the other. Shinozuka *et al.*[13] and Jangid[10], selected β by trial and error method, assuming that one objective does not vary much with significant variation in the other objective. As shown earlier, the optimal LRB designed through CWF approach may not yield the desired performance under different ground motions.

Hence to overcome the limitations of the CWF approach, this study evaluates suitable β for each hazard level through total error minimization method. The term 'error' here denotes the total deviation of the responses involved in both objectives with respect to their prespecified allowable limits. The underlying assumption of this approach is that the economic loss is minimum as long as the performance objectives are within their specified limits and the loss follows a linear trend once the individual objectives exceed these limits. The economic loss due to damage of the superstructure (including secondary components) and isolator is assumed to be of the same order. Therefore, the present analysis puts a constraint on the total deviation due to both PIDR and PBD to avoid severe damage to the base-isolated structure. The total error for each hazard level is thus expressed as follows

$$E = E_{\text{PIDR}} + E_{\text{PBD}}, \tag{11}$$

where E_{PIDR} and E_{PBD} represent the error due to PIDR and PBD respectively, and are expressed as

$$E_{\text{PIDR}} = \begin{cases} 0, & \text{if } d_r \le d_{r|\text{lim}} \\ \dfrac{d_r}{d_{r|\text{lim}}} - 1, & \text{otherwise} \end{cases} \tag{12}$$

$$E_{\text{PBD}} = \begin{cases} 0, & \text{if } x_b \le x_{b|\text{lim}} \\ \dfrac{x_b}{x_{b|\text{lim}}} - 1, & \text{otherwise} \end{cases}. \tag{13}$$

The allowable limits of PIDR and PBD for a given hazard level are denoted as $d_{r|\text{lim}}$ and $x_{b|\text{lim}}$ respectively. According to FEMA-356 (ref. 23), for SMRF structures, the allowable limit of PIDR is taken as 0.7%, 2.5% and 5% for performance level of immediate occupancy (IO), life safety (LS) and collapse prevention (CP) respectively[3]. Similarly, the allowable range of PBD that satisfies the stability criteria for buckling/bulging for a given gravity load of the structures[8] and the mean displacement response spectra of 2% in 50 years hazard level is around 0.5–0.6 m. Therefore, the present analysis considers the limiting value of PBD as 0.5 m for all the LRB-isolated SMRF and BF structures.

The range of the other two characteristic parameters of LRB considered for optimal design (i.e. q and T_b/T_s) was chosen as $0.5 \text{ cm} \le q \le 5 \text{ cm}$ and $1 \le T_b/T_s \le 7$. These specified lower and upper bounds were calculated by taking $K_{\text{Init}}/K_{\text{py}} \approx 10$–$20$. These limits also satisfy the required design criteria for manufacturing and practical considerations as mentioned in Datta[3]. The basic steps for the calculation of optimum $\bar{F}_y$ of LRB are as follows.

(1) The mean and mean + SD values of PIDR and PBD for a set of ground motions (representing a particular hazard level) were evaluated for $0.02 \le \bar{F}_y \le 0.03$. These values were calculated for a given value of T_b/T_s and q within their specified range.

(2) The mean + SD values of PIDR and PBD were normalized with respect to their maximum value to scale both the objectives between 0 and 1.

(3) The values of $f(\bar{F}_y)$ were evaluated using eq. (9) by varying the β values between 0.25 and 0.95, with an increment of 0.1.

(4) For each value of β, the minimum $f(\bar{F}_y)$ was selected and their corresponding values of $\bar{F}_y$, PIDR and PBD were determined.

(5) The total error of both the objectives (i.e. PIDR and PBD) with respect to their specified allowable limits was calculated based on eq. (11).

(6) The value of β giving the minimum value of total error was selected. $\bar{F}_y$ corresponding to this β value is the optimal normalized yield strength of LRB for the given value of T_b/T_s and q. The respective values of PIDR and PBD are the response of the base-isolated structure having optimum LRB.

(7) Aforementioned steps (1) to (6) were repeated for different values of T_b/T_s to evaluate the optimal $\bar{F}_y$. Then the suitable range of T_b/T_s within the above-mentioned range was selected such that the total normalized error was within 5%.

(8) Steps (1) to (6) were again repeated for chosen values of q and T_b/T_s within their effective range and the

optimal $\bar{F}_y$ was calculated by varying the superstructure parameters such as flexibility and damping.

(9) Steps (1) to (8) were repeated for the hazard levels 2% in 50 years (MCE) and 10% in 50 years (DBE) to evaluate the optimal $\bar{F}_y$, such that the corresponding objectives (i.e. PIDR and PBD) were within the specified allowable limits.

Finally, the total normalized error from the proposed approach was compared with that of the CWF approach for varying hazard levels to understand the robustness of the former.

Optimal design

Prior to optimal design, the four-storey ($T_s = 0.74$ sec) base-isolated structure (Figure 4 *a*) was analysed for an arbitrarily selected ground motion, i.e. LA27 from 2% in 50 years of hazard level and considering $T_b/T_s = 3.4$ and $q = 5$ cm. Figure 6 *a–c* shows the time-history plots of ground acceleration for LA27 along with the base shear (normalized with respect to the total seismic weight of the frame) and bearing displacement. Three different values of $\bar{F}_y$ were considered. From Figure 6 *b*, one can notice that for all $\bar{F}_y$ values, the normalized base shear is reduced significantly in comparison to the fixed-base case, as expected. From Figure 6 *c*, it can be observed that with an increase in the rigidity of the isolator, i.e. increase in $\bar{F}_y$ from 0.1 (grey line) to 0.3 (thick black dash), PBD decreases from about 58 to 30 cm, while the reduction in peak base shear is negligible. Hence, it is important to optimize $\bar{F}_y$ while keeping the initial rigidity as well as other structural performance parameters in mind.

For optimal design, nonlinear time-history analyses of the four-storey base-isolated frame were performed to evaluate PIDR and PBD under all ground motions of 10% in 50 years and 2% in 50 years hazard levels. For different values of $\bar{F}_y$ (between 0.02 and 0.3) and for 20 ground motions of each hazard level, the mean and mean + SD values of PIDR and PBD were evaluated. This process was carried out for $q = 0.5$, 1, 2.5 and 5 cm. Figure 7 *a* and *c* shows the variation of mean + SD values of PIDR and PBD respectively, for 10% in 50 years of hazard level and for all q values considered. It can be observed from Figure 7 *a* that PIDR shows an initial decreasing trend before increasing as $\bar{F}_y$ increases. This initial decreasing trend is attributed to the high damping force when the velocity is large for smaller $\bar{F}_y$. This can be explained due to the fact that force transfer to the superstructure consists of damping and spring forces of the bearings. For smaller values of $\bar{F}_y$, the bearings render into nonlinear zone early and hence the velocity is more. Thus, the damping force transferred to the structure is greater compared to the spring force. However, for higher values of $\bar{F}_y$, the velocity of the bearing is not so high and the damping force transferred to the superstructure is nominal compared to the spring force transferred due to deformation of the bearing. This can be verified by plotting the velocity time history of the bearings with respect to the ground (Figure 7 *b*) for $\bar{F}_y = 0.01$ (grey line), 0.04 (blue line) and 0.10 (red dash). One can notice in this plot that as the $\bar{F}_y$ increases, the velocity decreases. Figure 7 *c* shows the other objective, i.e. PBD, which decreases with an increase in $\bar{F}_y$ for all hazard levels. Further, from Figure 7 *a* and *c*, one can notice that with the increase in q from 0.5 to 5 cm, the values of both PIDR and PBD increase in the considered range of $\bar{F}_y$. Hence the lowest value of q, i.e. 0.5 cm is found to be effective and this value of q satisfies the specified range of $K_{Init}/K_{py} \approx 10$ (refs 3, 7).

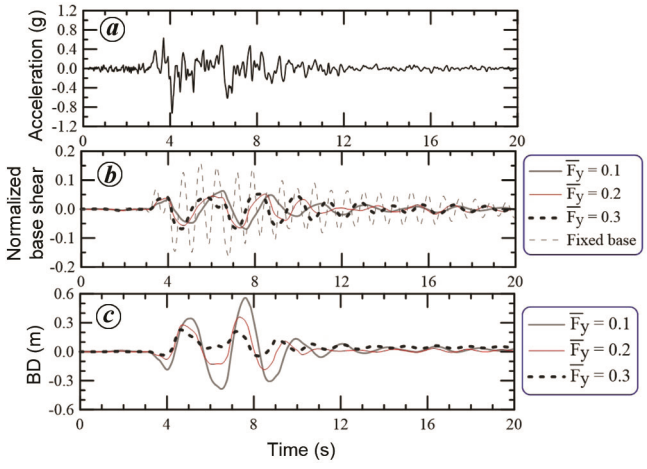

Figure 6. Time variation of (***a***) ground acceleration (LA27), and the corresponding (***b***) normalized base shear and (***c***) isolator displacement for different values of yield strength of LRB ($T_s = 0.74$ sec, $T_b/T_s = 3.4$ and $q = 5$ cm).

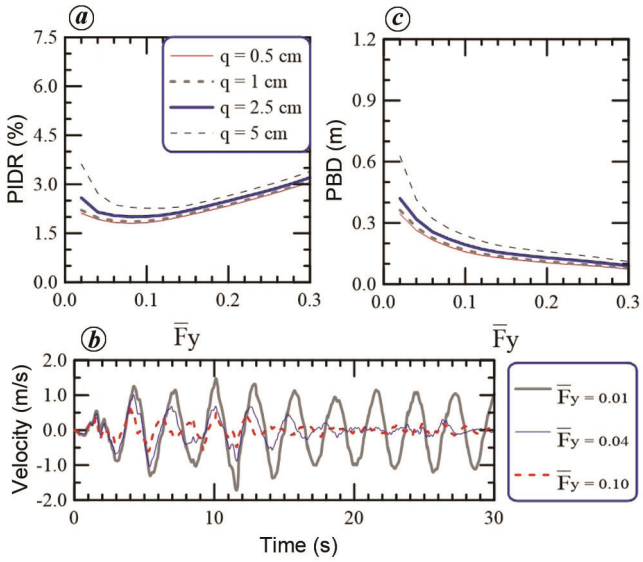

Figure 7. Variation of (***a***) PIDR and (***c***) PBD, and (***b***) velocity time history of isolator under ground motion LA01 ($T_s = 0.74$ sec and $T_b/T_s = 3.4$).

In the proposed approach, the value of β corresponding to the minimum value of total error (as evaluated from eq. (11)) has been considered for formulation. Hence, the individual errors due to each objective (from eqs (12) and (13)) are plotted in Figure 8 *a* and *b* for β values varying between 0.25 and 0.95, $T_b/T_s = 5.33$ and 2 respectively, and for ground motions of hazard level 2% in 50 years. The results show that the error is basically due to PBD for $T_b/T_s = 5.33$ (Figure 8 *a*), whereas for $T_b/T_s = 2$, the error is due to PIDR (Figure 8 *b*). For hazard level 10% in 50 years, the error is primarily due to PIDR and for higher values of T_b/T_s, both the objectives are within their specified limits. Therefore, the effective range of T_b/T_s for the chosen value q should be assessed prior to evaluation of optimum $\bar{F}_y$.

Effective range of post-yield isolation period

As mentioned earlier, the estimations of PIDR are already above the FEMA-356 (ref. 23) specified allowable limit for the values of q and T_b considered in the study of Jangid[10]. To avoid this situation (where structural drift exceeds the allowable limit) in the optimization process, the effective range of T_b/T_s needs to be assessed before computing the optimal $\bar{F}_y$. Thus, for different values of T_b/T_s between 1 and 7, the optimum $\bar{F}_y$ was evaluated for the four-storey stiff frame (taking $q = 0.5$ cm and steps as mentioned earlier) and is shown in Figure 9 *a* for both hazard levels. It is observed that the optimum $\bar{F}_y$ generally decreases with increase in the flexibility of LRB, and has larger values for ground motions of higher hazard levels. To compare these results with those of the CWF approach, a constant β value of 0.75 was considered in eq. (9). Figure 9 *b* shows the calculated values of optimal $\bar{F}_y$. One can notice that for $T_b/T_s \geq 3.5$, the variation of optimum $\bar{F}_y$ becomes almost insensitive and has nearly similar values for both hazard levels.

In order to study the effectiveness of the proposed approach, the normalized error corresponding to the proposed and CWF approaches is shown in Figure 10 *a* and *b* respectively. For the 2% in 50 years case, the effective range of T_b/T_s is between 3.25 and 5.75 as the total error is within 5%. This range is large (i.e. 2–7) for ground motions of 10% in 50 years hazard level (Figure 10 *a*). On the contrary, one can notice from Figure 10 *b* that no such effective range is found for 2% in 50 years hazard level, while for the 10% in 50 years case the effective range is less (i.e. 4–7) compared to the proposed approach. Further analysis reveals that that CWF approach results in considerable total error (approx. 60–75% higher than that of the proposed approach) for both hazard levels. The values of T_b/T_s considered for further calculations are somewhere in the range 3.25–5.75, as the total deviation of PIDR and PBD with respect to their specified limits is within 0–5%. As explained earlier, the values of β assessed using the proposed approach capture the relative importance of one objective with respect to the other for both hazard levels.

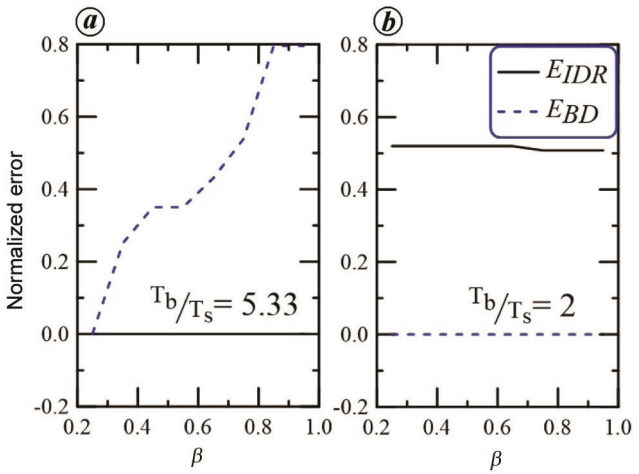

Figure 8. Estimated values of normalized error due to PIDR and PBD with β for ground motions of 2% in 50 years hazard level ($T_s = 0.74$ sec and $q = 0.5$ cm).

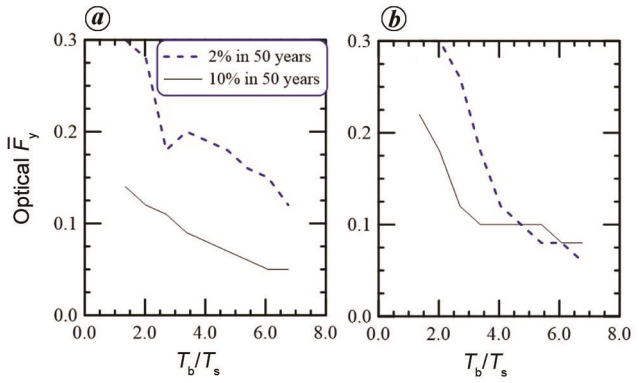

Figure 9. Variation of optimum $\bar{F}_y$ for a four-storey stiff frame using (***a***) variable and (***b***) constant weight factor approach ($q = 0.5$ cm).

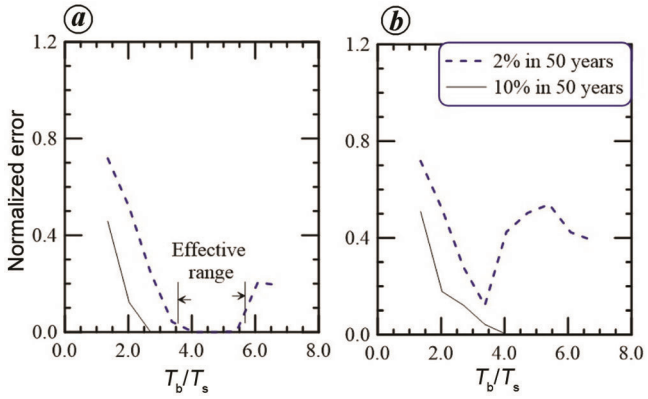

Figure 10. Variation of normalized error for a four-storey stiff frame using (***a***) variable and (***b***) constant weight factor approach ($q = 0.5$ cm).

Table 2. Variation of optimum $\bar{F}_y$ with the corresponding values of objectives, i.e. PBD and peak inter-storey drift ratio (PIDR) using variable weight factor approach for both hazard levels

Frame Column 1	T_s Column 2	Optimal $\bar{F}_y$ $T_b/T_s = 4$ Column 3	 $T_b/T_s = 6$ Column 4	PIDR (%) $T_b/T_s = 4$ Column 5	 $T_b/T_s = 6$ Column 6	PBD (m) $T_b/T_s = 4$ Column 7	 $T_b/T_s = 6$ Column 8
10% in 50 years							
Four-storey	0.73	0.08	0.06	1.72	1.27	0.23	0.30
Eight-storey	1.18	0.05	0.03	1.45	1.12	0.28	0.32
Sixteen-storey	1.85	0.03	0.02	1.49	0.97	0.32	0.37
Six-storey	1.17	0.06	0.05	2.50	2.38	0.29	0.32
Three-storey (BF)	0.66	0.08	0.06	1.91	1.85	0.34	0.36
2% in 50 years							
Four-storey	0.73	0.22	0.16	4.7	4.5	0.41	0.47
Eight-storey	1.18	0.14	0.12	2.57	2.29	0.43	0.45
Sixteen-storey	1.85	0.16	0.15	2.97	3.21	0.40	0.43
Six-storey	1.17	0.13	0.10	5.02	4.62	0.45	0.52
Three-storey (BF)	0.66	0.19	0.18	3.89	3.78	0.46	0.47

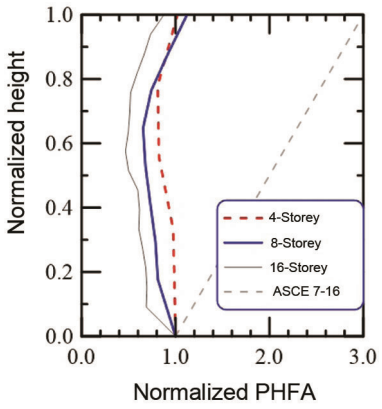

Figure 11. Mean + SD estimation of normalized PHFA of four-storey, eight-storey and sixteen-storey stiff SMRF structures with the code[21] specified allowable limits.

Optimum yield strength

The optimum yield strength of LRB was evaluated using the proposed approach for the considered pre-Northridge and contemporary code-designed structures. Table 2 shows the calculated values of optimum $\bar{F}_y$, PBD and PIDR for both hazard levels (for T_b/T_s = 4 and 6). The major findings from this study are as follows

- For a given type of frame of the pre-Northridge structures, with an increase in the number of storeys, the value of optimum $\bar{F}_y$ decreases (see columns 3 and 4 in Table 2). This implies that a less stiff isolator is effective as the force transferred to the superstructure reduces.
- For the six-storey frame, the optimum $\bar{F}_y$ of LRB using the variable weight factor approach is effective in restricting the total error within 5% for both hazard levels. The effective isolation periods for this optimally designed isolated frame are: (i) 3.19 sec ($T_b/T_s = 4$) and 3.48 sec ($T_b/T_s = 6$) for 10% in 50 years and (ii) 3.55 sec ($T_b/T_s = 4$) and 3.77 sec ($T_b/T_s = 6$) for 2% in 50 years hazard levels.
- For the three-storey BF structure, the LRB designed using the proposed approach is effective in reducing the structural responses with respect to the fixed-base outcomes and the specified damage parameters are well within the specified allowable limits. The effective isolation periods for this optimally designed isolated frame are: (i) 2.77 sec ($T_b/T_s = 4$) and 3.05 sec ($T_b/T_s = 6$) for 10% in 50 years and (ii) 2.91 sec ($T_b/T_s = 4$) and 3.18 sec ($T_b/T_s = 6$) for 2% in 50 years hazard levels.
- By comparing the optimum $\bar{F}_y$ for both 10% and 2% in 50 years hazard levels, it can be concluded that LRB with higher $\bar{F}_y$ is required to keep the structural (see columns 5 and 6 in Table 2) and isolator (see columns 7 and 8 in Table 2) parameters within the specified allowable limits of underground motions of higher intensity hazard levels.

The aforementioned points demonstrate that the proposed approach provides an efficient solution under varying hazard levels.

PHFA distribution for optimal cases

It is widely known that the behaviour of acceleration-sensitive secondary structures (often known as non-structural components/elements) appended to any floor of a building are characterized by the acceleration time history of that floor[4,21]. Hence, it is important to understand the distribution of PHFA in the case of optimal LRB (having $\bar{F}_y$ for $T_b/T_s = 4$ as given in Table 2) isolated frames with that of the code-specified design acceleration profile[17,21,22]. For this, the mean and mean + SD estimations of PHFA for each floor of the considered pre-Northridge

and contemporary code-designed structures with flexible base are evaluated. Figure 11 presents the mean + SD values of normalized PHFA for all pre-Northridge SMRF structures along with the ASCE-specified[21] design acceleration profile for floor acceleration. It may be noted that the distribution of normalized PHFA is well within the code-specified design distribution.

Conclusion

In this study we provide an approach to evaluate the optimal yield strength of LRB that is effective under ground motions of varying hazard levels. This has been achieved by taking code-specified performance objectives corresponding to each hazard level in the optimization formulation. In addition, a variable weight factor approach is proposed by giving proper weight to one objective with respect to the other, such that multiple performance objectives can be targeted. The proposed variable weight factor approach with the concept of minimization of total error is effective in the selection of optimal yield strength of LRB. Such effectiveness may be difficult to achieve for the conventional CWF approach. The LRB designed using the proposed approach is also effective in reducing the vulnerability of acceleration-sensitive non-structural components/elements appended to the frames, and structural members of both pre-Northridge and two contemporary code-designed structures.

The findings of this study, however, are limited to the parameter space, particularly, in terms of quantitative results (i.e. number and type of building, ground motion, isolator period, etc.) considered herein.

1. Buckle, I. and Mayes, R., Seismic isolation: history, application, and performance – a world view. *Earthq. Spectra*, 1990, **6**(2), 161–201; https://doi.org/10.1193/1.1585564
2. Deb, S. K., Seismic base isolation – an overview. *Curr. Sci*., 2004, **87**(10), 1426–1430; https://www.jstor.org/stable/24109483.
3. Datta, T. K., *Seismic Analysis of Structures*, John Wiley and Sons (Asia) Pte Ltd, Singapore, 2010.
4. Villaverde, R., *Fundamental Concepts of Earthquake Engineering*, CRC Press, Boca Raton, 2009, 1st edn.
5. Roy, T. and Matsagar, V., Multi-hazard analysis and design guidelines: recommendations for structure and infrastructure systems in the Indian context. *Curr. Sci.*, 2021, **121**(1), 44–55; https://doi:10.18520/cs/v121/i1/44-55
6. Roy, T. and Matsagar, V., Effectiveness of passive response control devices in buildings under earthquake and wind during design life. *Struct. Infrastruct. Eng.*, 2019, **29**(10), 2503–2513; https://doi.org/10.1080/15732479.2018.1547768
7. Liu, M., Burns, S. A. and Wen, Y. K., Multiobjective optimization for performance-based seismic design of steel moment frame structures. *Earthquake Eng. Struct. Dyn.*, 2005, **34**(3), 289–306; https://doi.org/10.1002/eqe.426
8. Naeim, F. and Kelly, J. M., *Design of Seismic Isolated Structures from Theory to Practice*, John Wiley, New York, 1999.
9. Chakraborty, S., Roy, K. and Ray-Chaudhuri, S., Design of re-centering spring for flat sliding base isolation system: theory and a numerical study. *Eng. Struct.*, 2016, **126**, 66–77; https://doi.org/10.1016/j.engstruct.2016.07.049
10. Jangid, R. S., Optimum friction pendulum system for near-fault motions. *Eng. Struct.*, 2005, **27**(3), 349–359; https://doi.org/10.1016/j.engstruct.2004.09.013
11. Zou, X. K., Integrated design optimization of base-isolated concrete buildings under spectrum loading. *Struct. Multidiscip. Optim*, 2008, **36**(5), 493–507; https://doi.org/10.1007/s00158-007-0184-5.
12. Zou, X. K., Chan, C. M., Li, G. and Wang, Q., Multiobjective optimization for performance-based design of reinforced concrete frames. *J. Struct. Eng.*, 2007, **133**(10), 1462–1474; https://doi.org/10.1061/(ASCE)0733-9445(2007)133:10(1462)
13. Shinozuka, M., Ray-Chaudhuri, S. and Mishra, S. K., Shape-memory-alloy supplemented lead rubber bearing (SMA-LRB) for seismic isolation. *Probab. Eng. Mech.*, 2015, **41**, 34–45; https://doi.org/10.1016/j.probengmech.2015.04.004
14. Santa-Ana, P. R. and Miranda, E., Strength reduction factors for multi-degree-of-freedom systems. In Proceedings of the 12th World Conference on Earthquake Engineering, Auckland, New Zealand, 2000, pp. 1–8.
15. FEMA-451, NEHRP recommended provisions: design examples. Federal Emergency Management Agency, Washington DC, USA, 2006.
16. Hossain, M. R., Ashraf, M. and Padgett, J. E., Risk-based seismic performance assessment of yielding shear panel device. *Eng. Struct.*, 2103, **56**, 1570–1579; https://doi.org/10.1016/j.engstruct.2013.07.032
17. ICBO, Structural engineering design provisions. International Conference of Building Officials, California, USA, 1994.
18. OpenSees, OpenSees – Open system for earthquake engineering simulation. Pacific Earthquake Engineering Research Center, California, USA, 2017; http://opensees.berkeley.edu/
19. Somerville, P., Smith, N., Punyamurthula, S. and Sun, J., Development of ground motion time histories for phase 2 of the FEMA/SAC steel project. Federal Emergency Management Agency, Washington DC, USA, 1997; http://www.sacsteel.org/project/
20. Skinner, R. I., Robinson, W. H. and McVerry, G. H., *An Introduction to Seismic Isolation*, Wiley Publishers, New York, 1993.
21. ASCE, Minimum design loads for buildings and other structures (ASCE/SEI 7-16). American Society of Civil Engineers, Reston, VA, USA, 2016.
22. NEHRP, NEHRP recommended provisions for seismic regulations for new buildings and other structures. National Earthquake Hazards Reduction Program, Building Seismic Safety Council, Washington DC, USA, 2000.
23. FEMA-356, Prestandard and commentary for the seismic rehabilitation of buildings. Federal Emergency Management Agency, Washington DC, USA, 2000.

ACKNOWLEDGEMENT. Financial support to Jagajyoti Panda by the Ministry of Education, Government of India and IIT Kanpur is greatly appreciated.

Received 23 August 2021; revised accepted 17 November 2021

doi: 10.18520/cs/v122/i1/77-86